IJE TRANSACTIONS B: Applications Vol. 32, No. 11, (November 2019) 1610-1619

International Journal of Engineering

Journal Homepage: www.ije.ir

Voltage Regulation of DC-DC Series Resonant Converter Operating in Discontinuous Conduction Mode: The Hybrid Control Approach

H. Afshang*, F. Tahami

Department of Electrical Engineering, Sharif University of Technology, Tehran, Iran

P A P E R I N F O

Paper history:
Received 01 June 2019
Received in revised form 23 August 2019
Accepted 12 September 2019

Keywords:
Series Resonant Converter
Discontinuous Conduction Mode
Voltage Regulation
Hybrid Control
Piecewise Affine System
Stability Analysis

A B S T R A C T

Dynamic modeling and control of dc-dc series resonant converter (SRC) especially when operating in discontinuous conduction mode (DCM) is still a challenge in power electronics. Due to semiconductors switching, SRC is naturally represented as a switched linear system, a class of hybrid systems. Nevertheless, the hybrid nature of the SRC is commonly neglected and it is modeled as a purely continuous dynamics based on the sinusoidal approximation and averaging. However, an SRC may be purposely designed to operate in DCM so the sinusoidal approximation is no longer acceptable. Therefore, it is essential to analyze the stability using a more sophisticated model. This paper presents a novel hybrid control strategy for the output voltage regulation of the SRC operating in DCM. Neither sinusoidal nor averaging is used. The stability of the closed-loop system is systematically fulfilled by satisfying some linear matrix inequalities. The proposed hybrid control approach has simple hardware implementation which does not require fast sampling of the resonant tank waveforms and external voltage-controlled oscillator. A prototype of the SRC is constructed and the hybrid controller is realized on a TMS320F2812 DSP core. The effectiveness of the proposed method is verified by simulation and experimental results.

***doi**: 10.5829/ije.2019.32.11b.12*

1. INTRODUCTION

Nowadays, using high-frequency power converters is inevitable in many applications. High frequencies are desirable since they result in smaller and lighter magnetic components and faster transient responses. However, the switching losses and electromagnetic interferences are major issues in these converters. Soft switched converters can overcome these restrictions by using zero current and/or voltage switching [1-4]. In consequence of these features and the ever-increasing demand for higher power density, higher efficiency and lower electromagnetic interference, resonant converters are currently of widespread interest and used in many industrial applications such as high voltage power supply for industrial magnetron [5], renewable energy applications [6], LED driver [7], automotive engine/battery hybrid power generators [8], driver of switched reluctance motors [9].

The subject of dynamic modeling and control of dc-dc series resonant converters is still a challenge in power electronics. Due to semiconductors switching, the SRC has a switched linear dynamics, which is a class of hybrid systems. Nevertheless, it is common that the hybrid nature of the SRC is neglected, and the SRC is modeled as a purely continuous dynamics based on the fundamental harmonic (sinusoidal) approximation [10-13] and generalized averaging theory [14]. This approximated model is nonlinear and usually, a linearized model around an operating point or a piecewise linear model in a region of state space is obtained [15, 16]. The main reason for such a simplification is to facilitate stability analysis and controller design.

For some specific applications such as industrial magnetron, microwave generator [17] and modern solid-state transformer [18], the SRC may be purposely designed to operate in DCM. Operation of the SRC in

*Corresponding Author: *hamid_afshang@ee.sharif.edu* (H. Afshang)

Please cite this article as: H. Afshang, F. Tahami, Voltage Regulation of DC-DC Series Resonant Converter Operating in Discontinuous Conduction Mode: The Hybrid Control Approach, International Journal of Engineering (IJE), IJE TRANSACTIONS B: Applications Vol. 32, No. 11, (November 2019) 1610-1619

DCM is well behaved, in that the output voltage increases monotonically with increasing the switching frequency and the switch turn-on and turn-off transitions both occur at zero current switchings (ZCS). The error resulting from the use of averaged-nonlinear/linearized model of the SRC operating in DCM for stability analysis and controller design is significant because the current and voltage of the resonant tank are very different from the sinusoidal shape and the fundamental harmonic approximation is no longer acceptable. It is shown in this paper that a classic PI controller which is designed based on the linearized model of the SRC not only does not guarantee the stability of the closed-loop system but also can even cause instability. Therefore, it is essential to investigate the stability analysis and controller design of the SRC using a more sophisticated model rather than common approximated models.

The hybrid modeling technique was presented in the literature as a natural representation of power electronic converters [19-21]. Piecewise affine (PWA) systems is a well-known and wide-applicable class of hybrid. By employing the PWA model, which consists of linear (or, rather, affine) subsystems, the stability analysis, and control design problems can be reduced to some linear matrix inequality (LMI) problems [22-27]. Based on the inherent switched linear dynamics of the SRC, the authors have already proposed hybrid control of the SRC operating above/below the resonance in continuous conduction mode (CCM) [28-30].

This paper presents a novel hybrid control strategy for the output voltage regulation of the SRC operating in DCM. The proposed hybrid controller is presented in two steps: In the first step, an innovative frequency modulator (FM) is provided so that the overall system resulting from the connection of the FM and the SRC has a PWA dynamics. In the second step, based on the stability theorem of the PWA systems a hybrid controller is designed for the SRC system So that the output voltage of the converter is regulated and the stability of the closed-loop system is guaranteed. The stability of the closed-loop system is systematically fulfilled by satisfying some linear matrix inequalities. The proposed hybrid control method has simple hardware implementation which does not require fast sampling of the resonant tank waveforms. Moreover, there is no need for VCO hardware. A prototype of the SRC is constructed and the hybrid controller is realized on a TMS320F2812 DSP core. The simulation and experimental results show the effectiveness of the proposed approach.

This paper is organized as follows: In Section 2 the switched linear model of the SRC is introduced. Section 3 discusses the hybrid controller and stability analysis of the closed-loop system. Section 4 provides the simulation and experimental results. Finally, the conclusion of the paper is presented.

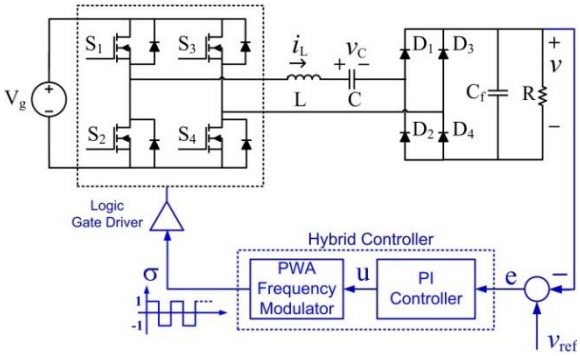

Figure 1. Schematic of the proposed hybrid control of the SRC

2. INHERENT SWITCHED LINEAR MODEL OF SRC

The schematic of the proposed hybrid control of the dc-dc series resonant converter is illustrated in Figure 1. The converter consists of a controlled switch network (full-bridge inverter), a series resonant tank, an uncontrolled rectifier, and a capacitive low-pass filter. The controllable switches S_1, S_2, S_3, and S_4 are controlled by a discrete input, $\sigma(t)$ to produce a square-wave voltage of frequency f_s in the series resonant tank input port. The tank with the resonant frequency of f_0 acts as a band-pass filter on this square-wave voltage, and then the tank current is rectified by a diode bridge. The high-frequency ripple of the output voltage is filtered by a capacitor to produce a pure dc voltage for the resistive load. By changing the switching frequency f_s, the magnitude of the tank ringing response can be modified, and hence the dc output voltage can be controlled.

Depending on the semiconductors ON/OFF state, the controlled switch network has two modes: 1) S_1, S_4 are ON and S_2, S_3 are OFF, 2) S_1, S_4 are OFF and S_2, S_3 are ON. And also, the uncontrolled diode rectifier has three modes: 1) D_1, D_4 are ON and D_2, D_3 are OFF, 2) D_1, D_4 are OFF and D_2, D_3 are ON, 3) all diodes become simultaneously reverse biased. Therefore, a total of six modes or subsystems can occur in an SRC while operating in DCM. Assuming that all components of the SRC are ideal, the circuit topologies for the six subsystems are as given in Figure 2. Each subsystem is a linear time-invariant network. Since the switching or transition from one subsystem to another is constrained to both controlled switch network and uncontrolled rectifier, two types of switching can be distinguished; 1) *controlled or external switching*, in which a transition is a result of changes of the discrete-input σ, 2) *uncontrolled or internal switching*, where a transition occurs when the converter continuous state variables satisfy certain conditions.

The switched linear model of the SRC can be described as:

$$\begin{cases} \frac{d}{dt}\begin{bmatrix} i_L \\ v_C \\ v \end{bmatrix} = \mathrm{A_q}\begin{bmatrix} i_L \\ v_C \\ v \end{bmatrix} + \mathrm{a_q} \\ q = \varphi(i_L, v_C, v, \sigma) \end{cases} \quad (1)$$

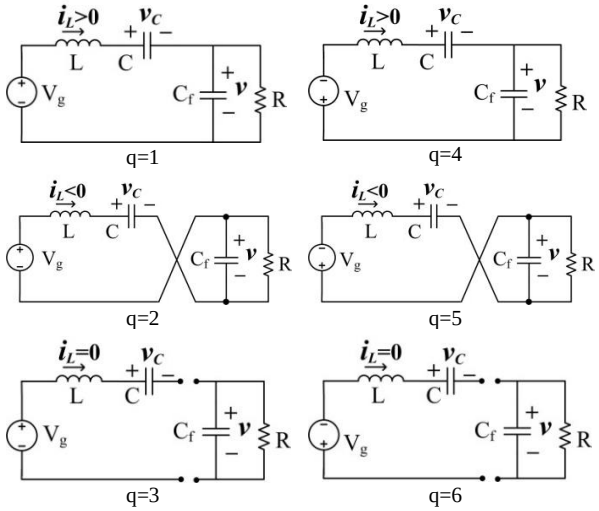

Figure 2. Circuit topologies for the six subsystems of SRC

TABLE 1. The constraints and matrices of each subsystem in Equation (1)

q	$\mathbf{A_q}$	$\mathbf{a_q}$	Constraints
1	$\begin{bmatrix} 0 & -\frac{1}{L} & -\frac{1}{L} \\ \frac{1}{C} & 0 & 0 \\ \frac{1}{C_f} & 0 & -\frac{1}{RC_f} \end{bmatrix}$	$\begin{bmatrix} \frac{V_g}{L} \\ 0 \\ 0 \end{bmatrix}$	$\sigma = +1$ $i_L > 0$
2	$\begin{bmatrix} 0 & -\frac{1}{L} & \frac{1}{L} \\ \frac{1}{C} & 0 & 0 \\ -\frac{1}{C_f} & 0 & -\frac{1}{RC_f} \end{bmatrix}$	$\begin{bmatrix} \frac{V_g}{L} \\ 0 \\ 0 \end{bmatrix}$	$\sigma = +1$ $i_L < 0$
3	$\begin{bmatrix} 0 & 0 & 0 \\ 0 & 0 & 0 \\ 0 & 0 & -\frac{1}{RC_f} \end{bmatrix}$	$\begin{bmatrix} 0 \\ 0 \\ 0 \end{bmatrix}$	$\sigma = +1$ $i_L = 0$ $\lvert V_g - v_C \rvert < v$
4	$\begin{bmatrix} 0 & -\frac{1}{L} & -\frac{1}{L} \\ \frac{1}{C} & 0 & 0 \\ \frac{1}{C_f} & 0 & -\frac{1}{RC_f} \end{bmatrix}$	$\begin{bmatrix} -\frac{V_g}{L} \\ 0 \\ 0 \end{bmatrix}$	$\sigma = -1$ $i_L > 0$
5	$\begin{bmatrix} 0 & -\frac{1}{L} & \frac{1}{L} \\ \frac{1}{C} & 0 & 0 \\ -\frac{1}{C_f} & 0 & -\frac{1}{RC_f} \end{bmatrix}$	$\begin{bmatrix} -\frac{V_g}{L} \\ 0 \\ 0 \end{bmatrix}$	$\sigma = -1$ $i_L < 0$
6	$\begin{bmatrix} 0 & 0 & 0 \\ 0 & 0 & 0 \\ 0 & 0 & -\frac{1}{RC_f} \end{bmatrix}$	$\begin{bmatrix} 0 \\ 0 \\ 0 \end{bmatrix}$	$\sigma = -1$ $i_L = 0$ $\lvert -V_g - v_C \rvert < v$

where the resonant tank inductor current i_L, capacitor voltage v_C, and the output voltage v are the continuous state variables. $\sigma(t)$ is the discrete-input (or logic-input) of the SRC, necessarily restricted to take values in the discrete set $\{+1, -1\}$. The index variable q determines the subsystem number. The function φ determines the current subsystem number which is constrained to the continuous state variables and the discrete input variable. The constraints and matrices of each subsystem are expressed in Table 1.

3. THE PROPOSED HYBRID CONTROL OF THE SRC

As discussed in the previous section, the SRC has a switched linear dynamics where the switching rule depends on both discrete input and continuous state variables. The stability analysis and control design of such hybrid systems are very difficult and not straightforward.

PWA systems are another class of hybrid systems which is similar to switched linear systems, with the exception that the switching rule depends only on the continuous state variables. Stability analysis and control design of PWA systems can be reduced to some linear matrix inequalities (LMI).

The proposed hybrid controller is presented in two steps: In the first step, an innovative frequency modulator is provided so that the overall system resulting from the connection of the FM and the SRC presents a PWA dynamics. In the second step, based on the stability theorems of PWA systems, an output feedback controller is designed so that the output voltage of the converter is regulated and the stability of the closed-loop system is guaranteed.

3. 1. Frequency Modulator with a PWA Dynamics

In this paper, an innovative FM with PWA dynamics is presented. It can be explained using the equivalent circuit as shown in Figure 3. It receives a continuous signal $u(\mathrm{t}) \in \mathbb{R}^+$ at the input and generates a square-wave signal $\sigma(\mathrm{t}) \in \{-1, +1\}$ at the output.

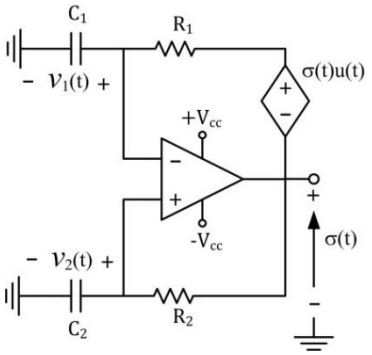

Figure 3. Equivalent circuit of the proposed FM

The evolution of the FM state variables during a switching period and the sequence of subsystems subintervals have been illustrated in Figure 4.

Mode 1: At the beginning of the first subinterval, assume that the comparator output is $+V_{cc}$ and the capacitors' initial voltages are $-V_{cc}$. Analysis of two RC circuits leads to the following results:

$$v_2(t) = V_{cc} - 2V_{cc}e^{-\frac{t}{\tau_2}} \quad (2)$$

$$v_1(t) = (1+u)V_{cc} - (2+u)V_{cc}e^{-\frac{t}{\tau_1}} \quad (3)$$

where $\tau_2 = R_2C_2$ and $\tau_1 = R_1C_1$. The FM circuit parameters R_1, R_2, C_1, C_2 are chosen so that τ_2 is much less than τ_1. In other words, $v_2(t)$ is dynamically faster than $v_1(t)$. The capacitor C_2 is charged faster than capacitor C_1. Thus C_2 is fully charged faster and ready for switching to the next mode. The voltage across C_1 tends towards $(1+u)V_{cc}$ as time passes. Just at the moment when $v_1(t)$ becomes higher than $v_2(t)$, the comparator output changes instantly to $-V_{cc}$ and the first subinterval ends.

Mode 2: At the beginning of the second subinterval, the comparator output is $-V_{cc}$ and the capacitors' initial voltages are $+V_{cc}$. Analysis of two RC circuits leads to:

$$v_2(t) = -V_{cc} + 2V_{cc}e^{-\frac{\left(t-\frac{T_s}{2}\right)}{\tau_2}} \quad (4)$$

$$v_1(t) = -(1+u)V_{cc} + (2+u)V_{cc}e^{-\frac{\left(t-\frac{T_s}{2}\right)}{\tau_1}} \quad (5)$$

The capacitor C_2 is discharged faster than capacitor C_1. Thus C_2 is fully discharged faster and ready for switching to the next mode. The voltage across C_1 drops exponentially from $+V_{cc}$ towards $-(1+u)V_{cc}$ as time passes. Just at the moment when $v_1(t)$ becomes lower than $v_2(t)$, the comparator output changes instantly to $+V_{cc}$ and the second subinterval ends.

This cycle is repeated continuously and a square-wave signal $\sigma(t)$ with a frequency of f_s is generated at the output of FM. The charging/discharging duration of the capacitor C_1 can be decreased by increasing the continuous input $u(t)$, and thus the frequency of $\sigma(t)$ can be increased. For two different values of $u(t)$, the waveforms of the FM are shown in Figure 5.

State-space model of the proposed FM with PWA dynamics is as follows:

$$\begin{cases} \frac{d}{dt}\begin{bmatrix} v_1 \\ v_2 \end{bmatrix} = \begin{bmatrix} -\frac{1}{\tau_1} & 0 \\ 0 & -\frac{1}{\tau_2} \end{bmatrix}\begin{bmatrix} v_1 \\ v_2 \end{bmatrix} + \sigma\left(\begin{bmatrix} \frac{1}{\tau_1} \\ \frac{1}{\tau_2} \end{bmatrix} + \begin{bmatrix} \frac{1}{\tau_1} \\ 0 \end{bmatrix}u\right) \\ \sigma = sgn(v_2 - v_1) \end{cases} \quad (6)$$

It is noteworthy that in this article, the electrical circuit of the proposed FM is not implemented using electronic devices, but its mathematical dynamical model has been implemented in a digital signal processor (DSP).

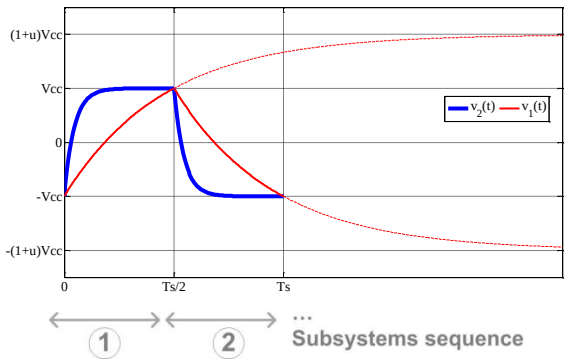

Figure 4. Evolution of the FM state variables during a switching period

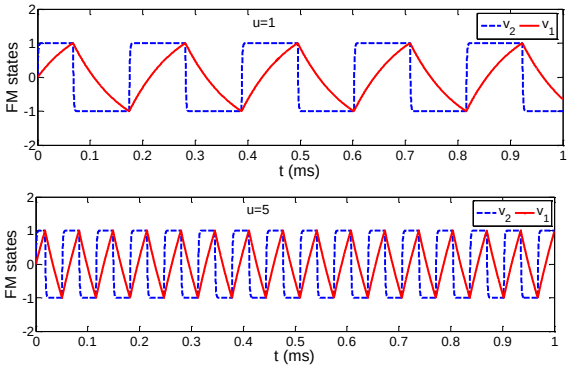

Figure 1. waveforms of the FM for two different values of u

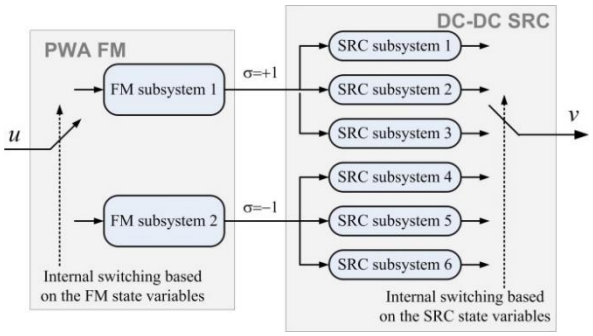

Figure 2. Block diagram of the FM-SRC connection

3. 2. FM-SRC Connection to Obtain a PWA System

Block diagram of the FM-SRC connection is shown in Figure 6. External switching of the SRC is equivalent to the internal switching of the FM.

Considering the internal switching of the FM and SRC, six modes or six forward paths from the input u to the output v can occur. For example, when $v_2 > v_1$ and $i_L < 0$, the first FM subsystem and the second SRC subsystem are activated. The overall system made from the FM input following by the SRC output has a piecewise affine dynamics that each subsystem has a linear (or, rather, affine) dynamics and the switching rule

from one subsystem to another is constrained only to the continuous state variables. By merging the switched linear model of the SRC in Equation (1) and PWA model of the FM in Equation (6), the PWA model of the total FM-SRC connection can be obtained as:

$$\frac{d}{dt}\begin{bmatrix} i_L \\ v_C \\ v \\ v_1 \\ v_2 \end{bmatrix} = A_q \begin{bmatrix} i_L \\ v_C \\ v \\ v_1 \\ v_2 \end{bmatrix} + a_q + b_q u \quad : for \begin{bmatrix} i_L \\ v_C \\ v \\ v_1 \\ v_2 \end{bmatrix} \in \chi_q \tag{7}$$

where χ_q is a region of the state space where q-th subsystem is valid. It can be represented as the intersection of finite numbers (p_q) of half-space. In other words, for each cell χ_q, there exists the identifier matrices G_q and g_q such that

$$\chi_q = \left\{ \begin{bmatrix} i_L \\ v_C \\ v \\ v_1 \\ v_2 \end{bmatrix} | \mathrm{G_q} \begin{bmatrix} i_L \\ v_C \\ v \\ v_1 \\ v_2 \end{bmatrix} + \mathrm{g_q} \succcurlyeq 0 \right\} \tag{8}$$

where $\mathrm{G_q}$ is a $\mathrm{p_q}$-by-n matrix and $\mathrm{g_q}$ is a $\mathrm{p_q}$-by-1 matrix. The inequality $\mathrm{z} \succcurlyeq 0$ means that all entries of the vector z are non-negative. The matrices $\mathrm{A_q}$, $\mathrm{a_q}$, $\mathrm{b_q}$, $\mathrm{G_q}$ and $\mathrm{g_q}$ are expressed as in Table 2.

3. 3. Closed-loop Control System of the SRC The block diagram of the output feedback control of the SRC is shown in Figure 7. To regulate the output voltage of the SRC, a PI controller with the following state- space model is considered:

$$\begin{cases} \dot{z} = \mathrm{e} \\ u = \mathrm{k_I} z + \mathrm{k_P} e \end{cases} \tag{9}$$

where z is the state variable of the PI controller, e is the regulation error of the SRC output voltage, $\mathrm{k_I}$ and $\mathrm{k_P}$ are the PI integrator and proportional coefficients, respectively. The overall system resulting from the connection of the PI controller and the PWA FM is called the *proposed hybrid controller* which is implemented on a DSP.

The PWA dynamics of the closed-loop control system of the SRC is as follows:

$$\frac{d}{dt}\begin{bmatrix} i_L \\ v_C \\ v \\ v_1 \\ v_2 \\ z \end{bmatrix} = \begin{bmatrix} \mathrm{A_q} - \mathrm{b_q k_P C} & \mathrm{b_q k_I} \\ -\mathrm{C} & 0 \end{bmatrix} \begin{bmatrix} i_L \\ v_C \\ v \\ v_1 \\ v_2 \\ z \end{bmatrix} + \begin{bmatrix} \mathrm{a_q} + \mathrm{b_q k_P v_{ref}} \\ \mathrm{v_{ref}} \end{bmatrix} \tag{10}$$

$$\text{for } \begin{bmatrix} i_L \\ v_C \\ v \\ v_1 \\ v_2 \\ z \end{bmatrix} \in \left\{ \begin{bmatrix} \mathrm{G_q} & 0_{\mathrm{p_q} \times 1} \end{bmatrix} \begin{bmatrix} i_L \\ v_C \\ v \\ v_1 \\ v_2 \\ z \end{bmatrix} + \mathrm{g_q} \succcurlyeq 0 \right\}$$

TABLE 2. The Values of Matrices in Equations (7) and (8)

q	$\mathbf{A_q}$	$\mathbf{a_q}$	$\mathbf{b_q}$	$\mathbf{G_q}$	$\mathbf{g_q}$
1	$\begin{bmatrix} 0 & \frac{-1}{L} & \frac{-1}{L} & 0 & 0 \\ \frac{1}{C} & 0 & 0 & 0 & 0 \\ \frac{1}{C_f} & 0 & \frac{-1}{RC_f} & 0 & 0 \\ 0 & 0 & 0 & \frac{-1}{\tau_1} & 0 \\ 0 & 0 & 0 & 0 & \frac{-1}{\tau_2} \end{bmatrix}$	$\begin{bmatrix} \frac{V_g}{L} \\ 0 \\ 0 \\ \frac{1}{\tau_1} \\ \frac{1}{\tau_2} \end{bmatrix}$	$\begin{bmatrix} 0 \\ 0 \\ 0 \\ \frac{1}{\tau_1} \\ 0 \end{bmatrix}$	$\begin{bmatrix} 1 & 0 & 0 & 0 & 0 \\ 0 & 0 & 0 & -1 & 1 \end{bmatrix}$	$\begin{bmatrix} 0 \\ 0 \end{bmatrix}$
2	$\begin{bmatrix} 0 & \frac{-1}{L} & \frac{1}{L} & 0 & 0 \\ \frac{1}{C} & 0 & 0 & 0 & 0 \\ \frac{-1}{C_f} & 0 & \frac{-1}{RC_f} & 0 & 0 \\ 0 & 0 & 0 & \frac{-1}{\tau_1} & 0 \\ 0 & 0 & 0 & 0 & \frac{-1}{\tau_2} \end{bmatrix}$	$\begin{bmatrix} \frac{V_g}{L} \\ 0 \\ 0 \\ \frac{1}{\tau_1} \\ \frac{1}{\tau_2} \end{bmatrix}$	$\begin{bmatrix} 0 \\ 0 \\ 0 \\ \frac{1}{\tau_1} \\ 0 \end{bmatrix}$	$\begin{bmatrix} -1 & 0 & 0 & 0 & 0 \\ 0 & 0 & 0 & -1 & 1 \end{bmatrix}$	$\begin{bmatrix} 0 \\ 0 \end{bmatrix}$
3	$\begin{bmatrix} 0 & 0 & 0 & 0 & 0 \\ 0 & 0 & 0 & 0 & 0 \\ 0 & 0 & \frac{-1}{RC_f} & 0 & 0 \\ 0 & 0 & 0 & \frac{-1}{\tau_1} & 0 \\ 0 & 0 & 0 & 0 & \frac{-1}{\tau_2} \end{bmatrix}$	$\begin{bmatrix} 0 \\ 0 \\ 0 \\ \frac{1}{\tau_1} \\ \frac{1}{\tau_2} \end{bmatrix}$	$\begin{bmatrix} 0 \\ 0 \\ 0 \\ \frac{1}{\tau_1} \\ 0 \end{bmatrix}$	$\begin{bmatrix} 0 & -1 & 1 & 0 & 0 \\ 0 & 1 & 1 & 0 & 0 \\ 1 & 0 & 0 & 0 & 0 \\ -1 & 0 & 0 & 0 & 0 \\ 0 & 0 & 0 & -1 & 1 \end{bmatrix} \begin{bmatrix} V_g \\ -V_g \\ 0 \\ 0 \\ 0 \end{bmatrix}$	
4	$\begin{bmatrix} 0 & \frac{-1}{L} & \frac{-1}{L} & 0 & 0 \\ \frac{1}{C} & 0 & 0 & 0 & 0 \\ \frac{1}{C_f} & 0 & \frac{-1}{RC_f} & 0 & 0 \\ 0 & 0 & 0 & \frac{-1}{\tau_1} & 0 \\ 0 & 0 & 0 & 0 & \frac{-1}{\tau_2} \end{bmatrix}$	$\begin{bmatrix} \frac{-V_g}{L} \\ 0 \\ 0 \\ \frac{-1}{\tau_1} \\ \frac{-1}{\tau_2} \end{bmatrix}$	$\begin{bmatrix} 0 \\ 0 \\ 0 \\ \frac{-1}{\tau_1} \\ 0 \end{bmatrix}$	$\begin{bmatrix} 1 & 0 & 0 & 0 & 0 \\ 0 & 0 & 0 & 1 & -1 \end{bmatrix}$	$\begin{bmatrix} 0 \\ 0 \end{bmatrix}$
5	$\begin{bmatrix} 0 & \frac{-1}{L} & \frac{1}{L} & 0 & 0 \\ \frac{1}{C} & 0 & 0 & 0 & 0 \\ \frac{-1}{C_f} & 0 & \frac{-1}{RC_f} & 0 & 0 \\ 0 & 0 & 0 & \frac{-1}{\tau_1} & 0 \\ 0 & 0 & 0 & 0 & \frac{-1}{\tau_2} \end{bmatrix}$	$\begin{bmatrix} \frac{-V_g}{L} \\ 0 \\ 0 \\ \frac{-1}{\tau_1} \\ \frac{-1}{\tau_2} \end{bmatrix}$	$\begin{bmatrix} 0 \\ 0 \\ 0 \\ -\frac{1}{\tau_1} \\ 0 \end{bmatrix}$	$\begin{bmatrix} -1 & 0 & 0 & 0 & 0 \\ 0 & 0 & 0 & 1 & -1 \end{bmatrix}$	$\begin{bmatrix} 0 \\ 0 \end{bmatrix}$
6	$\begin{bmatrix} 0 & 0 & 0 & 0 & 0 \\ 0 & 0 & 0 & 0 & 0 \\ 0 & 0 & \frac{-1}{RC_f} & 0 & 0 \\ 0 & 0 & 0 & \frac{-1}{\tau_1} & 0 \\ 0 & 0 & 0 & 0 & \frac{-1}{\tau_2} \end{bmatrix}$	$\begin{bmatrix} 0 \\ 0 \\ 0 \\ \frac{-1}{\tau_1} \\ \frac{-1}{\tau_2} \end{bmatrix}$	$\begin{bmatrix} 0 \\ 0 \\ 0 \\ \frac{-1}{\tau_1} \\ 0 \end{bmatrix}$	$\begin{bmatrix} 0 & -1 & 1 & 0 & 0 \\ 0 & 1 & 1 & 0 & 0 \\ 1 & 0 & 0 & 0 & 0 \\ -1 & 0 & 0 & 0 & 0 \\ 0 & 0 & 0 & 1 & -1 \end{bmatrix} \begin{bmatrix} -V_g \\ V_g \\ 0 \\ 0 \\ 0 \end{bmatrix}$	

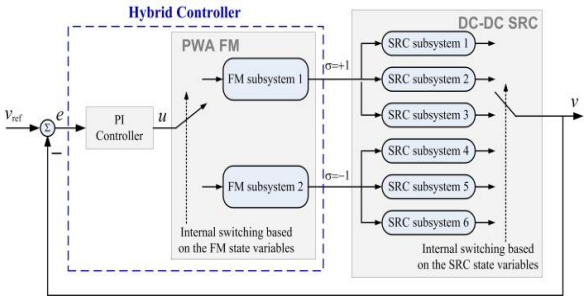

Figure 7. Block diagram of the closed-loop control system of the SRC

where $C = [0 \quad 0 \quad 1 \quad 0 \quad 0]$.

Thanks to the stability theorem of the PWA systems [22-24], the stability analysis of the closed-loop control system of the SRC can now be performed as follows: Consider the symmetric matrices P_q, U_q and W_q such that U_q, and W_q have non-negative entries. If the matrices P_q, U_q and W_q can be found such that the following inequalities are satisfied

$$P_q - \begin{bmatrix} G_q & 0_{p_q \times 1} & g_q \end{bmatrix}^T W_q \begin{bmatrix} G_q & 0_{p_q \times 1} & g_q \end{bmatrix} > 0 \qquad (11)$$

$$\begin{bmatrix} A_q - b_q k_P C & b_q k_I & a_q + b_q k_P v_{ref} \\ -C & 0 & v_{ref} \\ 0_{1\times 5} & 0 & 0 \end{bmatrix}^T P_q + P_q \begin{bmatrix} A_q - b_q k_P C & b_q k_I & a_q + b_q k_P v_{ref} \\ -C & 0 & v_{ref} \\ 0_{1\times 5} & 0 & 0 \end{bmatrix} + \begin{bmatrix} G_q & 0_{p_q \times 1} & g_q \end{bmatrix}^T U_q \begin{bmatrix} G_q & 0_{p_q \times 1} & g_q \end{bmatrix} < 0 \qquad (12)$$

then the stability of the closed-loop control system of the SRC is ensured. The values of PI controller coefficients (k_I, k_P) are obtained by solving the above LMIs in the form of the convex optimization problem in MATLAB.

3. 4. Comparison of Different Control Methods

A qualitative comparison between the proposed hybrid method and other methods for closed-loop control of the SRC is presented in Table 3.

Based on the first harmonic approximation of the resonant tank waveforms and the dc component approximation of the output voltage, the averaged model of the SRC is obtained as follows:

$$\frac{dV(t)}{dt} = \frac{\frac{8V_g}{\pi^2 C_f}}{\sqrt{\left(\frac{8}{\pi^2}R\right)^2 + \left(2\pi f_s(t) L - \frac{1}{2\pi f_s(t) C}\right)^2}} - \frac{1}{RC_f} V(t) \qquad (13)$$

where $V(t)$ is the average value of the output voltage in a switching period. This averaged model is a nonlinear system with purely continuous dynamics. Stability analysis and controller design for such a system are not straightforward. That's why perturbation and linearization around a steady-state operating point are common among engineers. The linearization can be accomplished using the Taylor expansion. The transfer function of the linearized model will be as follows:

$$G_{SRC}(s) = \frac{K}{s+P} \qquad (14)$$

$$K = \frac{8V_g}{\pi^2 C_f} \frac{\left(2\pi L + \frac{1}{2\pi C f_s^2}\right)\left(\frac{1}{2\pi C f_s} - 2\pi L f_s\right)}{\left[\left(\frac{8}{\pi^2}R\right)^2 + \left(2\pi L f_s - \frac{1}{2\pi C f_s}\right)^2\right]^{\frac{3}{2}}}, \quad P = \frac{1}{RC_f}$$

In the next section, it is shown that a PI controller, which is designed based on the linearized model of the SRC, not only does not guarantee the stability of the closed-loop system but also can even cause instability.

TABLE 3. Comparison of Different Control Methods

Approach	Approximation	SRC Conduction Mode	Stability Analysis Method
Averaged Nonlinear	first-harmonic averaging	CCM	Direct Lyapunov (difficult)
Averaged Linear	first-harmonic averaging small-signal	CCM	indirect Lyapunov (simple)
DPWA	no	CCM	Systematic using LMI
Proposed Hybrid Control	no	CCM and DCM	Systematic using LMI

TABLE 4. The Values of DC-DC SRC Parameters

Symbol	Quantity	Value
V_g	input voltage	60V
V_{ref}	desired output voltage	30V
L	resonant tank inductor	48μH
C	resonant tank capacitor	200nF
C_f	output filter capacitor	47μF
f_0	resonant frequency	51.4kHz
R_0	tank characteristic impedance	15.5Ω
R	load resistance	20Ω

4. SIMULATION AND EXPERIMENTAL RESULTS

A closed-loop control system of the SRC is simulated in MATLAB for verification of the proposed hybrid control method. The specifications and design values of the major components of the SRC are summarized in Table 4.

The following hybrid controller has been designed based on the proposed approach in the previous section:

$$\begin{cases} \frac{dz}{dt} = e \\ u = 2862.1z + 2.7e \\ \frac{d}{dt}\begin{bmatrix} v_1 \\ v_2 \end{bmatrix} = \begin{bmatrix} -1.0273\times 10^4 & 0 \\ 0 & -10^7 \end{bmatrix}\begin{bmatrix} v_1 \\ v_2 \end{bmatrix} \\ +sgn(v_2 - v_1)\left(\begin{bmatrix} 1.0273\times 10^4 \\ 10^7 \end{bmatrix} + \begin{bmatrix} 1.0273\times 10^4 \\ 0 \end{bmatrix} u\right) \\ \sigma = sgn(v_2 - v_1) \end{cases}$$

4. 1. Simulation Results Output voltage regulation at the presence of load change and input voltage disturbance are shown in Figures 8 and 9, respectively. The switching frequency, resonant tank inductor current, and capacitor voltage are also shown. In Figure 8, the load resistance is arbitrarily changed from 20 to 15 Ω and one can see that the output voltage is regulated within 1.5 ms. In Figure 9, the input voltage varies from 60 to 50 V and the output voltage is regulated

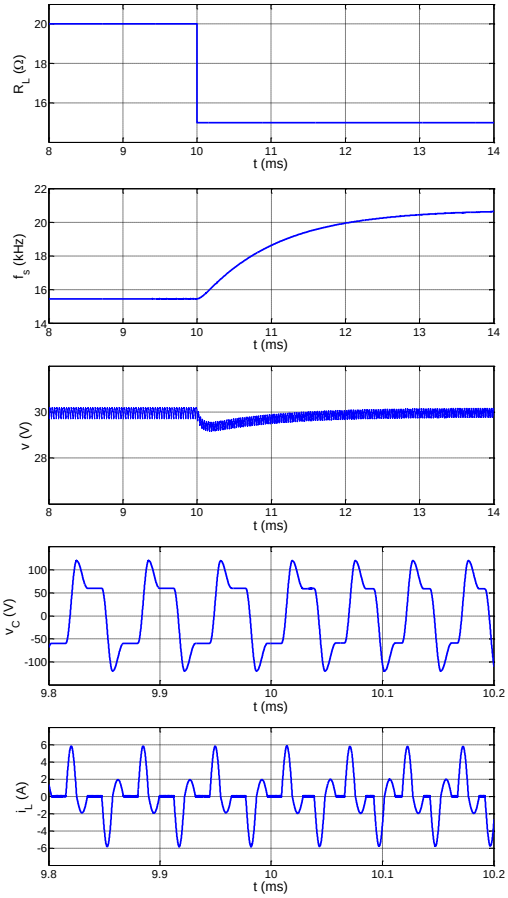

Figure 8. Simulated waveforms during load variation

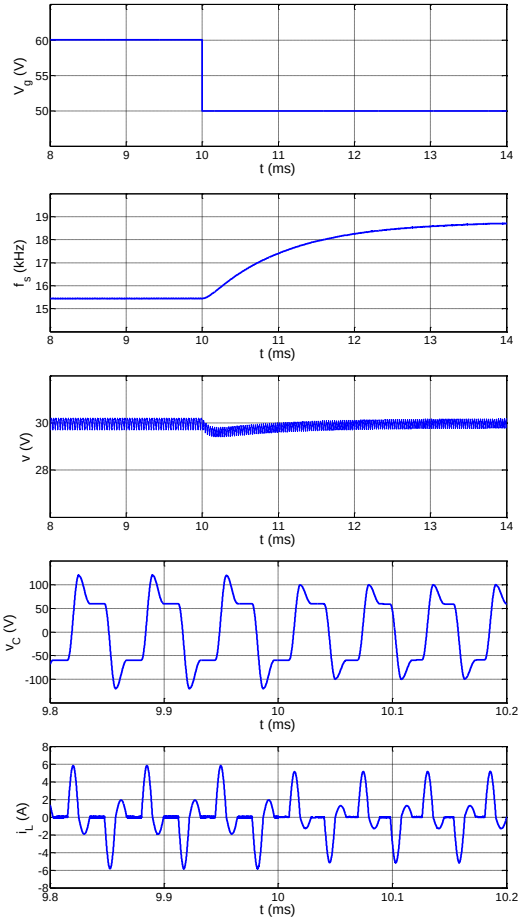

Figure 9. Simulated waveforms during input voltage variation

within 1.2 ms. Suitable steady-state response and good voltage stability under variations of load resistance and input voltage are observed from the simulation results.

Based on the parameter values given in Table 4 and Equation (14), the transfer function of the linearized model of the SRC is as follows:

$$G_{SRC}(s) = \frac{1.4474}{S+1063.8}$$

It is obvious that in a closed-loop system with the unity negative feedback structure, the following PI controller meets the goals of closed-loop stability and output regulation for the above-mentioned first-order system.

$$G_{PI}(s) = \left(1.382 + \frac{73.5}{s}\right) \times 10^5$$

Now, the PI controller designed based on the linearized model of the SRC is used with the inherent switched linear model to simulate the response of the closed-loop system. The simulation results shown in Figure 10 indicate that the closed-loop system is unstable. The switching frequency becomes more and more, and the SRC output voltage and the resonant tank signals tend to zero. It can be concluded that a PI controller that is designed based on the linearized model of the SRC not only does not guarantee the stability of the closed-loop system but also can even cause instability.

This simulation highlights the importance of stability analysis in the proposed hybrid method.

4. 2. Experimental Results For better verification of the proposed control strategy, an experimental prototype has been designed and implemented as shown in Figure 11. The proposed hybrid controller has been implemented on a TMS320F2812 DSP core.

After the startup, the output voltage is regulated at 30 V and the steady-state tracking error is zero as shown in Figure 12(a). The steady-state tank inductor current and capacitor voltage are shown in Figure 12(b). As can be seen in this figure, in each switching half-cycle, there is a time interval that the resonant tank inductor current is zero. Turn off of all transistors that occur at this time interval in the ZCS condition.

The output voltage regulation at the presence of the load resistance variation from 20 Ω to 15 Ω is shown in

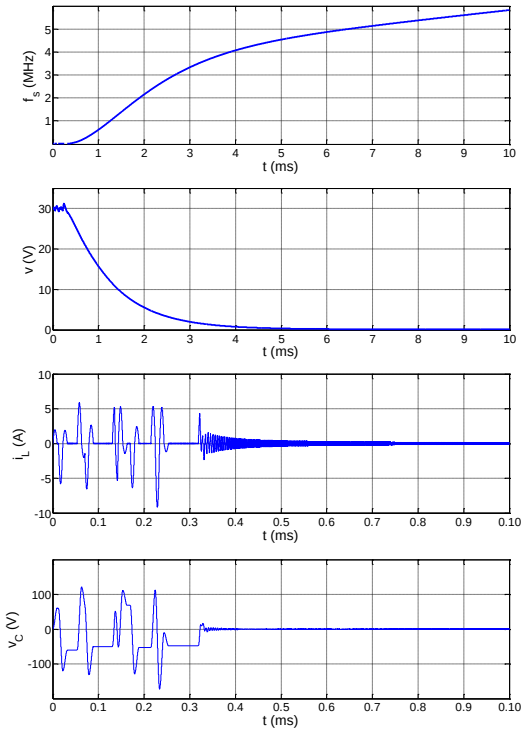

Figure 10. Instability of the closed-loop system for a PI controller which has been designed based on the linearized model of SRC

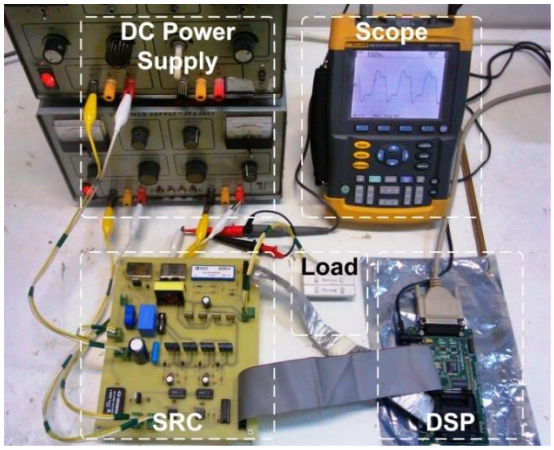

Figure 11. The experimental prototype of the proposed hybrid control of the SRC

Figure 13(a). The output voltage is compensated in about 1.5 ms. After compensating, both the steady-state tank inductor current and capacitor voltage are shown in Figure 13(b). Comparing with Figure 12(b), the switching frequency increased and the peak magnitudes of the tank inductor current and capacitor voltage did not change; which conforms to the simulation results.

The disturbance rejection of the proposed control method is also evaluated by a step change in the input voltage from 60 to 50 V while the load resistance is fixed at 20 Ω. As can be seen in Figure 14(a) the output voltage is compensated in about 1.2 ms. After compensating, the tank inductor current and capacitor voltage in the steady-state are shown in Figure 14(b). Comparing with Figure

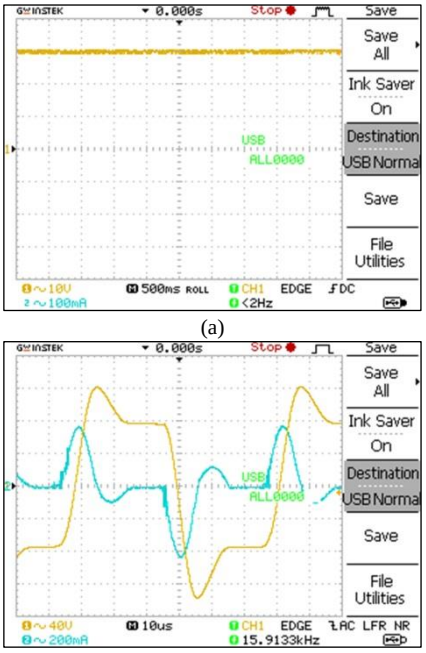

Figure 12. a) Output voltage is regulated at 30 V, b) steady-state resonant tank waveforms after startup, 1:$v_C(t)$ 2:$(0.625/8)i_L$

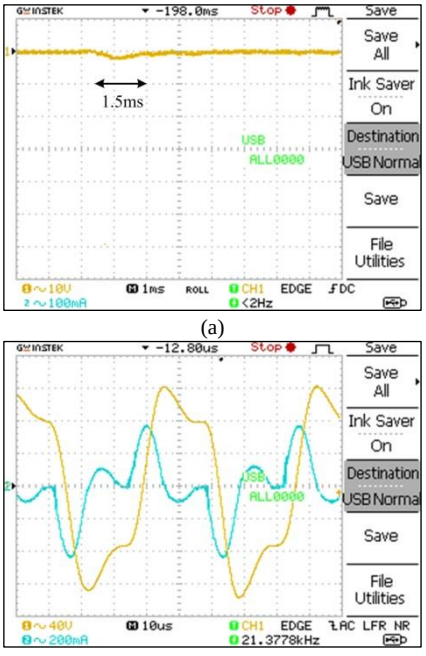

Figure 13. a) Output voltage of the SRC during load resistance change from 20 to 15 Ω, b) steady-state resonant tank waveforms after load change, 1:$v_C(t)$ 2:$(0.625/8)i_L$

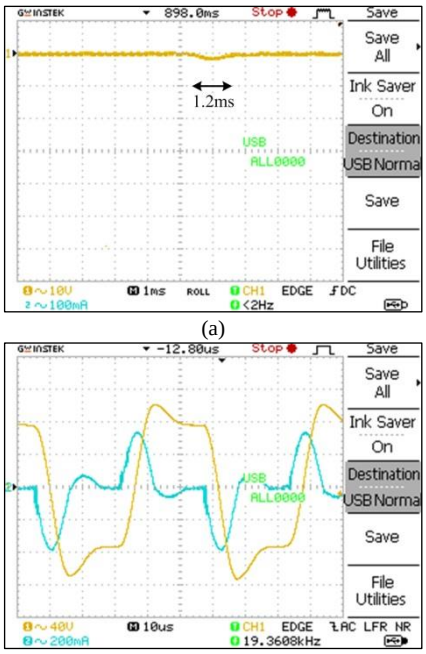

Figure 14. a) Output voltage of the SRC during input voltage change from 60 to 50 V, b) steady-state resonant tank waveforms after input voltage change, $1{:}v_C(t)$ $2{:}(0.625/8)i_L$

12(b), the switching frequency increased and the peak values of the tank waveforms decreased; which conforms to the simulation results.

5. CONCLUSION

In this article, the main focus was on Lyapunov stability of the closed-loop control system of the SRC when the converter operated in discontinuous conduction mode with zero current switchings. A novel frequency modulator was proposed so that the overall system resulting from the connection of the FM and the SRC has a PWA dynamics. Based on the PWA systems theory, a stabilizer hybrid controller was designed for the SRC voltage regulator. The simulation and experimental results showed that the proposed hybrid control method has a suitable steady-state response and good voltage stability under variations of load resistance and input voltage. For other converters that have different methods of soft-switching (Valley switching, Natural or extended ZVS, or Quasi-resonant ZCS/ZVS), if one can design an appropriate modulator so that the overall system resulting from connection of modulator and converter has a PWA dynamics, then Lyapunov stability of the closed-loop control system of that converter can be analyzed using PWA systems theory.

6. REFERENCES

1. Subramanian, N., "Analysis and experimentation of soft switched interleaved boost converter for photovoltaic applications", ***International Journal of Engineering Transaction A:* Basics**, Vol. 28, No. 10, (2015), 1469-1475.
2. Nair, M., "Simulation and experimental verification of closed loop operation of buck/boost dc-dc converter with soft switching", ***International Journal of Engineering C: Aspects***, Vol. 25, No. 4, (2012), 267-274.
3. Kazimierczuk, M.K. and Czarkowski, D., "Resonant power converters, John Wiley & Sons, (2012).
4. Erickson, R.W. and Maksimovic, D., "Fundamentals of power electronics, Springer Science & Business Media, (2007).
5. Jang, S.-R., Ryoo, H.-J., Ahn, S.-H., Kim, J. and Rim, G.H., "Development and optimization of high-voltage power supply system for industrial magnetron", ***IEEE Transactions on Industrial Electronics***, Vol. 59, No. 3, (2011), 1453-1461.
6. Krishnaswami, H. and Mohan, N., "Three-port series-resonant dc–dc converter to interface renewable energy sources with bidirectional load and energy storage ports", ***IEEE Transactions on Power Electronics***, Vol. 24, No. 10, (2009), 2289-2297.
7. Nerone, L.R., "Autoswitching led driver", ***IEEE Transactions on Power Electronics***, Vol. 27, No. 8, (2012), 3834-3842.
8. Park, J. and Choi, S., "Design and control of a bidirectional resonant dc–dc converter for automotive engine/battery hybrid power generators", ***IEEE Transactions on Power Electronics***, Vol. 29, No. 7, (2013), 3748-3757.
9. Afjei, E., "A new resonant converter circuit for reluctance", ***International Journal of Engineering***, Vol. 12, No. 2, (1999), 69-80.
10. Sanders, S.R., "On limit cycles and the describing function method in periodically switched circuits", ***IEEE Transactions on Circuits and Systems I: Fundamental Theory and Applications***, Vol. 40, No. 9, (1993), 564-572.
11. Liu, F., Chen, Y. and Chen, X., "Comprehensive analysis of three-phase three-level lc-type resonant dc/dc converter with variable frequency control—series resonant converter", ***IEEE Transactions on Power Electronics***, Vol. 32, No. 7, (2016), 5122-5131.
12. Wang, C.-S., Zhang, S.-h., Wang, Y.-f., Chen, B. and Liu, J.-h., "A 5-kw isolated high voltage conversion ratio bidirectional cltc resonant dc–dc converter with wide gain range and high efficiency", ***IEEE Transactions on Power Electronics***, Vol. 34, No. 1, (2018), 340-355.
13. Hu, S., Li, X. and Bhat, A.K., "Operation of a bidirectional series-resonant converter with minimized tank current and wide zvs range", ***IEEE Transactions on Power Electronics***, Vol. 34, No. 1, (2018), 904-915.
14. Sanders, S.R., Noworolski, J.M., Liu, X.Z. and Verghese, G.C., "Generalized averaging method for power conversion circuits", ***IEEE Transactions on Power Electronics***, Vol. 6, No. 2, (1991), 251-259.
15. Kazimierczuk, M.K. and Wang, S., "Frequency-domain analysis of series resonant converter for continuous conduction mode", ***IEEE Transactions on Power Electronics***, Vol. 7, No. 2, (1992), 270-279.
16. Park, H.-P. and Jung, J.-H., "Modeling and feedback control of llc resonant converters at high switching frequency", ***Journal of Power Electronics***, Vol. 16, No. 3, (2016), 849-860.
17. Kwon, S.-K., Saha, B., Mun, S.-P., Nishimura, K. and Nakaoka, M., "Series resonant zcs-pfm dc-dc converter using high frequency transformer parasitic inductive components and

lossless inductive snubber for high power microwave generator", ***Journal of Power Electronics***, Vol. 9, No. 1, (2009), 18-25.

18. Rothmund, D., Huber, J.E. and Kolar, J.W., "Operating behavior and design of the half-cycle discontinuous-conduction-mode series-resonant-converter with small dc link capacitors", in 2013 IEEE 14th Workshop on Control and Modeling for Power Electronics (COMPEL), IEEE., (2013), 1-9.
19. Goebel, R., Sanfelice, R.G. and Teel, A.R., "Hybrid dynamical systems", ***IEEE Control Systems Magazine***, Vol. 29, No. 2, (2009), 28-93.
20. Matthew, S., Gabriel, E. and Koo, T.J., Hybrid modeling and control of power electronics, in Hybrid systems: Computation & control. 2003, Springer-Verlag.450-465.
21. Mariéthoz, S., Almér, S., Bâja, M., Beccuti, A.G., Patino, D., Wernrud, A., Buisson, J., Cormerais, H., Geyer, T. and Fujioka, H., "Comparison of hybrid control techniques for buck and boost dc-dc converters", ***IEEE Transactions on Control Systems Technology***, Vol. 18, No. 5, (2009), 1126-1145.
22. Johansson, M.K.-J., "Piecewise linear control systems: A computational approach, Springer, Vol. 284, (2003).
23. Bemporad, A., Ferrari-Trecate, G. and Morari, M., "Observability and controllability of piecewise affine and hybrid systems", ***IEEE Transactions on Automatic Control***, Vol. 45, No. 10, (2000), 1864-1876.
24. Rodrigues, L. and Boyd, S., "Piecewise-affine state feedback for piecewise-affine slab systems using convex optimization", ***Systems & Control Letters***, Vol. 54, No. 9, (2005), 835-853.
25. Tahami, F. and Molaei, B., "Piecewise affine system modeling and control of pwm converters", ***Journal of Circuits, Systems, and Computers***, Vol. 16, No. 01, (2007), 113-128.
26. Tahami, F., Poshtkouhi, S. and Ahmadian, H.M., "Piecewise affine control design for power factor correction rectifiers", ***Journal of Power Electronics***, Vol. 11, No. 3, (2011), 327-334.
27. Nejadpak, A. and Tahami, F., "Stabilizing controller design for quasi-resonant converters described by a class of piecewise linear models", ***IEEE Transactions on Circuits and Systems I: Regular Papers***, Vol. 61, No. 1, (2013), 312-323.
28. Molla-Ahmadian, H., Karimpour, A., Pariz, N. and Tahami, F., "Hybrid modeling of a dc-dc series resonant converter: Direct piecewise affine approach", ***IEEE Transactions on Circuits and Systems I: Regular Papers***, Vol. 59, No. 12, (2012), 3112-3120.
29. Molla-Ahmadian, H., Tahami, F., Karimpour, A. and Pariz, N., "Hybrid control of dc–dc series resonant converters: The direct piecewise affine approach", ***IEEE Transactions on Power Electronics***, Vol. 30, No. 3, (2014), 1714-1723.
30. Afshang, H., Tahami, F. and Molla-Ahmadian, H., "Hybrid control of the dc–dc src operating below resonance", ***IET Power Electronics***, Vol. 10, No. 1, (2017), 1-9.

Voltage Regulation of DC-DC Series Resonant Converter Operating in Discontinuous Conduction Mode: The Hybrid Control Approach

H. Afshang, F. Tahami

Department of Electrical Engineering, Sharif University of Technology, Tehran, Iran

P A P E R I N F O

Paper history:
Received 01 June 2019
Received in revised form 23 August 2019
Accepted 12 September 2019

Keywords:
Series Resonant Converter
Discontinuous Conduction Mode
Voltage Regulation
Hybrid Control
Piecewise Affine System
Stability Analysis

چکیده

مدل‌سازی و کنترل مبدل‌های تشدیدی سری به ویژه هنگام کارکرد در وضعیت هدایت ناپیوسته جریان، هنوز یک چالش در الکترونیک قدرت می‌باشد. به خاطر کلیدزنی نیمه‌هادی‌ها، مبدل ذاتاً دارای دینامیک خطی سوئیچ‌شونده است که کلاس خاصی از سیستم‌های دورگه (هایبرید) محسوب می‌شود. از آنجایی که تحلیل پایداری و طراحی کنترل برای چنین مدلی دشوار است، معمولاً با استفاده از تقریب هارمونیک اول (سینوسی) و متوسط‌گیری، یک مدل پیوسته در زمان بدست می‌آورند که غیرخطی است و سپس آن را خطی‌سازی می‌کنند. در حالی که برای برخی از کاربردها، مبدل تشدیدی سری در زیر فرکانس تشدید و در وضعیت هدایت ناپیوسته جریان کار می‌کند که در این شرایط دیگر تقریب سینوسی قابل قبول نیست. بنابراین برای تحلیل پایداری به یک مدل دقیق‌تر نیاز است. در این مقاله یک استراتژی کنترل هایبرید جدید برای تنظیم ولتاژ خروجی مبدل تشدیدی سری هنگام کارکرد در وضعیت هدایت ناپیوسته جریان ارائه می‌شود. پایداری سیستم کنترل حلقه-بسته بطور سیستماتیک با استفاده از نامساوی‌های ماتریسی تضمین می‌شود. یک نمونه آزمایشگاهی از مبدل ساخته شده و کنترل‌کننده هایبرید پیشنهادی بر روی پردازشگر سیگنال دیجیتال TMS320F2812 پیاده‌سازی می‌شود. نتایج شبیه‌سازی و تست‌های آزمایشگاهی، کارآیی روش کنترل هایبرید پیشنهادی را تأیید می‌کنند.

***doi**: 10.5829/ije.2019.32.11b.12*